Improvement of curcumin solubility by polyethylene glycol/chitosan-gelatin nanoparticles (CUR-PEG/CS-G-nps).

Poopak Farnia[1,2], Saeed Mollaei[3], Afshin Bahrami[1], Alireza Ghassempour[4], Ali Akbar Velayati[1], Jalaledin Ghanavi[1,2]*

[1]Mycobacteriology Research Center, National Research Institute of Tuberculosis and Lung Disease (NRITLD), Shahid Beheshti University of Medical Sciences, Tehran, Iran

[2]Experimental Medicine and Tissue Engineering Center, National Research Institute of Tuberculosis and Lung Disease (NRITLD), Masih Daneshvari Hospital, Shahid Beheshti University of Medical Sciences, Tehran, Iran

[3]Department of Chemistry, Faculty of Science, Azarbaijan Shahid Madani University, Tabriz, Iran

[4]Department of Phytochemistry, Medicinal Plant and Drug Research Institute, Shahid Beheshti University, G. C., Evin, Tehran, Iran

Abstract

Curcumin (CUR), a yellow polyphenol compound is reportedly associated with a diverse therapeutic potential. Despite all curative properties of CUR, its usage in oral administration is restricted due to low bioavailability, low aqueous solubility and poor absorption rate. The aim of this study was to develop a nontoxic nanocurcumin (CUR-NPs) with enhanced bioavailability. For this reason, the CUR was first capped by polyethylene glycol (PEG) and then encapsulated into chitosan-gelatin nanoparticles (CS-G NPs). The PEG act as a co-solvent and CS-G act as a drug carrier biodegradable polymer. The efficiency and solubility of nanocurcumin were determined by transmission electron microscopy (TEM), fourier transformed infrared spectroscopy (FT-IR), dynamic light scattering (DLS) and high liquid chromatography (HPLC). Under TEM, the nanocurcumin were spherical in shape with average size of 300-400 nm. Zeta potential was 43.23 mV with 69.29% entrapment at 17.11% loading capacity. The solubility rate increased up to 2000 fold. The in-vitro drug release profile at PH 3.4 and PH 7.2 indicated a slow and controlled release at a constant rate. The release-rate is affected by size and loading capacity of NPs. In summary, the bioavailability of CUR-NPs was improved. Additionally, our procedure represents a mild and safety process for synthesizing efficient CUR-NPs, as we have not use any organic or toxic solvents.

Introduction

Curcumin (CUR), a bioactive component of turmeric (*Curcuma longa L.)* can interact with multiple targets to prevent diseases progression safely and inexpensively. They exhibit a wide range of pharmacological activities such as anti-inflammatory [1], anti-carcinogenic [2], anti-diabetic [3], antifungal and antiviral properties [4]. CUR is very effective against cancer cells like breast, prostate, head and neck cancers [5-7]. Although CUR reported to have many medicinal qualities, but due to poor aqueous solubility and poor bioavailability, its clinical application has been restricted [8-10]. To overcome the CUR limitations, researchers proposed the use of co solvency and nano drug carrier, which may represent the most practical approaches for improving the solubility of CUR in pharmaceutical liquid formulations

[11-15]. Generally, co solvents are the mixtures of miscible solvents that enhance the solubility of nonpolar solutes [12]. Among studied solvents that used as a co-solvent mixture, the polyethylene glycol (PEG), and propylene glycol (PG) gained more scientific attention. The polyethylene glycol (PEG) is a biocompatible, biodegradable, hygroscopic, stable, non-toxic and water-soluble liquid with bacteriostatic and fungistatic properties. Because of very low toxicity of PEG, it is an ideal medium for the topical delivery of many oral and parenteral drugs in animals and humans, as well as the formulations of fragrances, cosmetics and personal care products [13]. In recent years, *nanotechnology-based drug delivery systems* have aimed to transfer the drugs directly into target cells with more systematic and release control profile [14,15]. In this regards, many studies underline the importance of using chitosan (CS) and gelatin (G) as a nanodrugs carriers. Chitosan (CS) is a

linear polysaccharide composed of randomly distributed B-(*1-4*) *linked* D-glucosamine and N-acetyl-D-Glucosamine. It is soluble in acid solution and contains free amino groups. This compound is a biocompatible, non-toxic, and bio-resorbable polymer with biological activities, including antimicrobial activity [16,17]. Chitosan, also could open the tight junction between cells, thus enhancing the performance of drugs through mucosal tissues [18,19]. Gelatin (G), another carrier drug, was derived from type I collagen and is the primary component of the extracellular matrix in the eye and the skin. It is a low cost, biocompatible, biodegradable, resorbable, non-immunogenic under physiological conditions, and it has mechanical properties that can be modulated [20]. Furthermore, CS and G have been used together as potential carrier in drug delivery systems. Subramanian et al. (2014) demonstrated the use of CS-S composite as transdermal carrier for systemic delivery of drug via the skin [21]. Consequently, other investigators showed the preparation of CUR-CS-G composite at the various ratios of CS and G. This complex had antibacterial activity, and could improve wound closure and healing, respectively [22]. Despite these beneficial usage, CUR in CS-G composite showed low solubility. Thereby, in this study, we tried to increase the solubility of CUR by using polyethylene glycol (PEG) as a co-solvent system. Then, we loaded the CUR-PEG complex on CS-G NPs that were produced from glycerol 3-phosphate (GP). Thereafter, the drug release profile of the CUR-PEG loaded CS-G NPs were determined under different *in-vitro* conditions.

Experimental (Theory, Modelling)

Analytical HPLC analysis: For high liquid chromatography (HPLC) analysis, the Knauer (Germany) with binary HPLC pumps, diode array detector at 425 nm, column oven and a C18 column (Eruspher, 250 × 4.6 mm, 5 μm, 100 A°) was used. The CUR was eluted isocratically at flow rate of 1 ml/min using mobile phase concentration of acetonitrile and water (70:30, v/v) at room temperature. Injection volume was 20 μl and retention time of CUR was 5 min. The method was sensitive with a lower limit of quantitation of 5 ng/ml, with good linearity (r>0.996) over the linear range 5-10000 ng/ml. *The relative standard deviation* (RSD) was less than 5 % over the selected range. All the validation data, i.e., as accuracy and precision, were within the required limits.

Preparation of CS-G NPs

The CS-G NPs particles were prepared by a modification of our previous reports [23-26]. Briefly, CS solutions (3%) dissolve in 1% acetic acid and then added to a G solution (1% w/v). These solutions remained stirring at 37°C for 2 h. To produce CS-G NPs, the GP solution (1 and 3% w/v) also dissolved in 1% acetic acid and then added drop-wise to final solution under stirring for 2h duration.

Preparation of CUR-PEG loaded on CS-G NPs

One hundred milligram of CUR (100 mg) dissolved in 5ml of PEG solution (80%) as discussed previously [23]. Then under a

constant magnetic stirring (2 hours), the CUR-PEG complex was added drop-wise into CS-G NPs solutions. Thereafter, NPs were centrifuged (10000 rpm) for 10 min and then was stored at -80°C for future analysis.

Fourier transform infrared (FT-IR) spectroscopy

The samples were analyzed by FT-IR spectroscopy using a Perkin Elmer infrared spectrometer (model FT-PC-160). The samples were prepared as KBr pellets, using 40 scans and a resolution of 4 cm^{-1}.

Nano-encapsulation efficiency

The nano-encapsulation efficiency was determined by addition of one ml of acetonitrile into 2 mg of lyophilized NPs (to destroy the structure of NPs and release CUR). The concentration of released CUR was calculated by comparing the calibration curve with curve obtained from standard CUR. The % of entrapment efficiency and loading capacity were determined according to following equations:

Entrapment efficiency (%): [(CUR encapsulated /CUR total) ×100].

Loading capacity (%): [(CUR encapsulated /Nps total)×100].

Size measurement and determination of zeta potential

In order to measure the size and zeta potential of the CUR-loaded CS-G NPs, the samples were analyzed by dynamic light scattering (DLS) using zetasizer (Nano-ZS; Malvern Instruments, Malvern, UK). The transmission electron microscopy (TEM), (JEM1010-JEOL) was used to examine and compare the topography of the NPs.

Solubility of CUR

The solubility of CUR was determined in 4 different solutions including distilled water, PEG (20%), PEG (50%), and PEG (80%). The excess amount of CUR was added to a test tube containing 1ml of above mentioned solutions, separately. The solutions were stirred for 1 hour in a water bath (60°C) and centrifuged at 3000 rpm for 20 min. The supernatant was collected and analyzed by HPLC. The solubility of the CUR-PEG loaded on CG-G NPs was also determined in same way as it was used by distilled water as a solvent.

In-vitro release studies

The *in vitro* drug release of CUR from NPs was evaluated using dialysis membrane method. The obtained CUR-PEG loaded on CS-G NPs (5 mg) were suspended in 5 ml of buffer solution (pH 3.6 and 7.2) and were put into a dialysis bag with cut-off 14 KD. The dialysis bag was immersed in 50 ml of buffer solution (pH 3.60 and 7.20) at 37°C with continuous stirring. To keep the volume constant, one hundred micro liter (100 μl) of the samples withdrawn at predetermined time interval and immediately replaced with an equal volume of dissolution medium. The final release of CUR was obtained using HPLC method.

Results

Solubility studies

The solubility of CUR was determined by HPLC method using calibration curve. The solubility profile of CUR (10 g/ml) in water was very low. As shown in figure 1(tube A), most of CUR particles remain precipitated and undissolve in water (Figure 1A). Although, addition of PEG to the CUR, increases the solubility (50 mg/ml) up to 80% (Figure 1B). The CUR-PEG loaded on CS-G NPs showed more dissociation in water at an even higher concentration (about 20 mg/ml) (Figure 1C). The suspension from CUR-PEG loaded on CS-G NPs had natural yellow in colour, which indicates incorporation of CUR into the NPs dispersion.

Figure 1. *Images showing (A) CUR suspended in distilled water, (B) CUR dissolved in PG (80%), and (C) aqueous suspension of CUR-PEG loaded on CS-G NPs*

FT-IR Analysis

Figure 2 exhibits the FT-IR spectra of, (a) CS, (b) G, (c) CUR, and (d) CUR-loaded CS-G NPs. The FT-IR spectrum of CS indicated five characteristic peaks. The –OH stretching is manifested through peaks at 3443 cm^{-1}, while peaks at 2923, 1636 and 1382 cm^{-1} correspond to the CH stretching, NH$_2$ group and the CO stretching of the primary alcoholic group, respectively. The peak in the region 1071 cm^{-1} is due to the C-O-C stretching group [27]. The FT-IR spectrum of G showed three major peak regions marked as Amide A and B (3600-2700 cm^{-1}), Amide I, II and III (1900-900 cm^{-1}), and Amide IV, V and VI (400-900 cm^{-1}). Amide-I band (1700-1600 cm^{-1}) is the most sensitive spectral region to the protein secondary structure [28]. The CUR spectrum exhibits a broad peak at 3417 cm^{-1} may be due to the presence of bonded OH stretching of phenols and the strong peak at 1641 cm^{-1} predominantly mixed (C =C) and (C =O) character. Another strong band at 1583 cm^{-1} is attributed to the symmetric aromatic ring stretching vibrations (C= C). The 1511 cm^{-1} ring peak is assigned to the (C=O), while enol C-O peak was obtained at 1276 cm^{-1}, C- O-C peak at 1030 cm^{-1}, benzoate trans-CH vibration at 959 cm^{-1} and cis CH vibration of aromatic ring at 713 cm^{-1} [29]. Evidence of CUR-loaded CS-G NPs formation comes from the appearance of the bands, which indicates that there is an interaction between these compounds. In the spectra of CUR-loaded CS-Gelatin NPs, a peak at 1640

cm^{-1} was observed which corresponds to –NH deformation and a change in the peak at 1051 cm^{-1} correspond to keto group of the CUR.
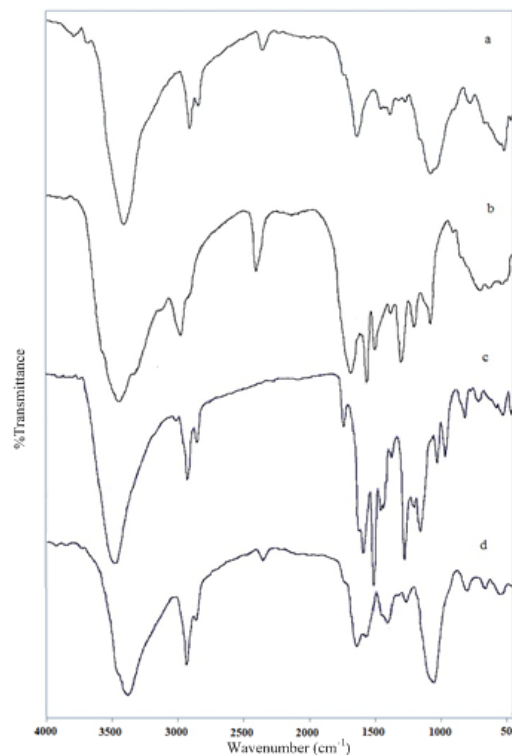

Figure 2. *FT-IR spectra of (a) CS, (b) G, (c) CUR and (d) CUR-loaded CS-G NPs.*

Physico-chemical characterization of CUR-PEG loaded on CS-G NPs

The particle size data of the CUR-PEG loaded on CS-G NPs with different concentration of the GP (1 and 3) were shown in Table 1 and the typical size distribution of the NPs is illustrated in figure 3, respectively. It was observed that the particle size decreased from 334 nm to 264 nm with the increase of GP concentration (Figures 3A1 and A2). The TEM image of the CUR-PEG loaded on CS-G NPs indicates that the NPs has spherical morphology with particle size about 360 nm for CS-G-GP (3:1:1 w/w/w %) and 270 nm for CS-G-GP (3:1:3 w/w/w %) (Figures 3B1 and B2). These results are consistent with DLS results. As shown table 1, the amount of the zeta potential of the cationic group of CUR-loaded CS-G NPs were increased from 21 mV to 43 mV when the concentration of the GP was increased from 1 to 3%. This indicated that the GP interacted electrostatically with the CS-G which in turn decreased the positive charges of this complex to form CS-GP-G NPs. Also, the GP concentration was significantly affected on the encapsulation efficiency and changed from 44% to 69%. So, higher concentration of the GP was caused higher encapsulation efficiency. Moreover, increasing the GP concentration increased loading capacity from 15% to 17%. Therefore, from above data, we concluded that the

encapsulation efficiency and loading capacity increased with increasing GP concentration.

Table 1. *Physicochemical properties of NPs.*

Particle type	Z-average (nm) n=3, ± SD	PDI●	Zeta potential (mV)	Cur loading (%) (w/w)	Encapsulation efficiency (%)
A1	264.21 ± 17.09	0.06	+23.49	15.31	44.04
B2	334.19 ± 20.52	0.11	+43.23	17.11	69.29

● high polydispersity index

1 A: The ratio of CS, G and GP in the NPs is 3:1:1 (v/v/v %) respectively

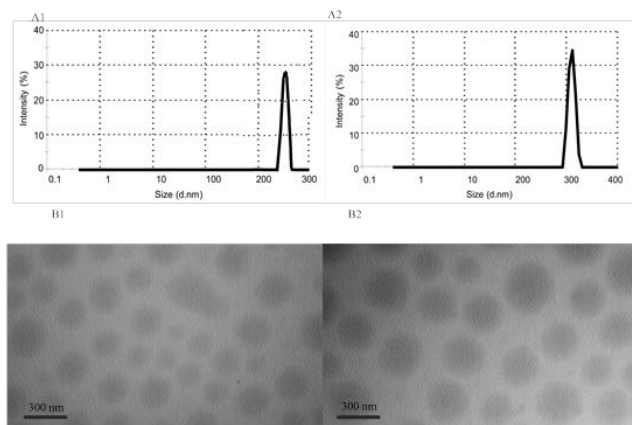2 B: The ratio of CS, G and GP in the NPs is 3:1:3 (v/v/v %) respectively

Figure 3. *DLS measurement and TEM image of CS-G NPs with different concentration of GP. The ratio of CS, G and GP was 3, 1, 1 (v/v/v %) at A1 and B1, and 3, 1, 3 (v/v/v %) at A2 and B2, respectively.*

In vitro release studies

The release of CUR from nano-encapsulated CUR was determined under in- vitro condition (at pH 3.4 and 7.2). All release behavior lasted for more than 48 hours. It indicated that the CUR-PEG loaded on CS-G NPs showed a good performance of drug controlled release. Furthermore, all release profiles of the NPs exhibit a slow release at constant rate. As shown in figure 4, the release of CUR was faster in acidic pH (3.4) than in neutral (pH: 7.2). Moreover, we noticed that the drug release behavior with different concentration of the GP, at constant pH, is different. In the case of CS-G-GP (3:1:1 w/w/w %), at pH 3.4, the release of the CUR from the dialysis bag started after 15 min which was 1,990 ng/ml; after 12 h and 24 h the release of CUR were 27,831 and 49,203 ng/ml, respectively; and at 48 h the concentration reached to 84,307 ng/ml. These results indicated that almost 7.7% CUR was released in 48 h (at pH 3.4). The CS-G-GP (3: 1: 3 w/w/w %) had the best results, so that the release of CUR was almost 1.7 fold of CS-G-GP (3:1:1 w/w/w %) (138,321 ng/mL after 48 h).
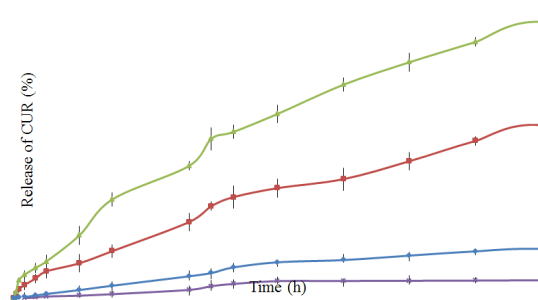

Figure 4. *Release profile of CUR from CUR-loaded CS-G NPs at different pH and GP concentration. The ratio of CS, G and GP in the NPs was (A1): 3, 1, 1 (v/v/v %), at pH 3.40, (A2): 3, 1, 1 (v/v/v %), at pH 7.20, (B1): 3, 1, 3 (v/v/v %), at pH 3.40, and (B2): 3, 1, 3 (v/v/v %), at pH 7.20, respectively.*

Table 2. *Release of CUR (mg) at different times.*

NO.	Carrier	Time			Ref.
		3 h (mg)	6 h (mg)	12 h (mg)	
*	Chitosan/Gelatin	0.4	0.6	1.2	*
1	Dextran sulphate/Chitosan	0.14	0.3	0.48	39
2	Poly-ε-Caprolactone	0.008	0.02	0.048	43
3	Chitosan	0.007	0.025	0.05	44
4	Chitosan/polycaprolactone	0.002	0.003	0.006	45
5	Chitosan/cyclodextrin	0.4	0.6	1.5	46
6	N-isopropylacrylamide /N-vinyl-2-pyrrolidone/ poly(ethyleneglycol)monoacrylate	3	2	1	47

*These results were taken from release of CUR from CS-G NPs (3: 1 w/w) according to our data.

Discussion

Generally, there are two main ways to get curcumin into our body; it can be used in its powdered form, or it can be

encapsulated with different composites. The oral bioavailability of curcumin, 'due to poor water solubility', is low. In oral administration they rapidly get clear off from the body and often a high dose is required to reach a therapeutic plasma concentration. These challenges would lower the clinical efficacy of CUR. It has been shown that the encapsulation of CUR with biodegradable nanoparticles can significantly improve curcumin's solubility and bioavailability. Few researchers used an organic solvent (i.e., chloroform) to improve solubility [30,31]. Although, such chlorinated solvents usually removed by evaporations, but a trace of them may remain in the final formulation of drugs, causes a potential risk for human health. Seedher and Bhatia [32] showed the enhanced solubility of celecoxib, rofecoxib and nimesulide by using a series of pure solvents and solvent mixtures. Water, alcohols, glycols, glycerol, and polyethylene glycol 400 (PEG 400) were used as solvents and water-ethanol, glycerol-ethanol, and polyethylene glycol-ethanol were used as mixed-solvent systems. They showed PEG 400-ethanol system had highest solubilization potential [32]. Others showed the increased in CUR solubility (20 mg/ml) by using a co-solvent system such as N-methyl pyrrolidinone, Tween 80, ethanol and water without any visual precipitation of the solid drug [33]. In the present study, we used PEG as co-solvent system. PEG has a very low toxicity and high biological activities. We showed that CUR solubility in PEG was increased about 2000-fold compared to CUR in water. Indeed, trapping of the CUR into PEG, might increases the CUR solubility. This mechanism has already been conceived between the CUR and other molecules such as phosphatidylcholine and starch [34,35]. They showed formation of hydrophobic interaction between CUR and phosphatidylcholine /or starch in addition to hydrogen bond. Recently, Wahlstrom and Blennow [36] documented poor absorption of CUR after its oral administration (1 g/kg) in rats. A negligible amount of Cur was found in blood plasma of fed rats, which proves its poor absorption from the gut. Thereby the other reason for poor bioavailability of CUR is their poor absorption. Few investigators showed the ability of CS to modulate structure of a tight junction between epithelial intercellular, thus enabling the better paracellular transport of drug molecules [18,19]. Here, we used a combination of PEG, chitosan (CS) and gelatin (G) for producing curcumin nanoparticles. This complex may improve both absorption and bioavailability of the Cur, together. Taravel and Domard [37,38] showed that interactions between chitosan and gelatin are made by both electrostatic and hydrogen bonding. In fact, chitosan biopolymer has considerable number of hydroxyl and –NH^{+3} groups that they can interact with hydrogen bond in gelatin. Moreover, the –NH^{+3} groups of chitosan can electrostatically interacted with oppositely charged –COO$^-$ groups of gelatin. As a result, a repulsive force formed between –NH^{+3} charges of chitosan and gelatin that will prevent further interaction. To overcome this repulsive force, chitosan is added to neutralize charges by decreasing the amount of free –NH^{+3} groups and increasing hydrogen bonding which consequently reduces the electrostatic repulsion. Thus, the CS–G NPs were spontaneously formed by mixing equal volume of GP solution to CS-G solution. The CUR -PEG loaded on CS–G NPs, by

constant stirring at 37°C. The CUR-PEG could be connected to CS-G NPs by hydrophobic (aromatic ring and diene structure) and hydrophilic (the phenolic OH, the o-methoxy groups and dione structure) interactions. The formation of CUR -loaded CS-G NPs complex was confirmed by FT-IR analysis, as reported by other [29]. Usually, the stability, enhanced permeability and retention effect of NPs is determined by size distribution, surface charge of NPs and zeta potential value, respectively. The surface of CUR-loaded NPs had high positive value (>30mv), indicated a net positive charges. This could represent a strong repellent force among particles that prevents aggregation of the NPs and resulted in more uniform size distribution in stable suspension on water. In a sense, the value of zeta potential represents an index for particle stability. Our results showed that in higher concentration of GP, the value of zeta potential increased, whereas the NPs sizes reduced (Table1). Our finding indicates a direct relation between loading capacity and entrapment efficiency with GP concentration. The CUR release from NPs was slow release at a constant rate. Although, the rate of release was more at acidic conditions than neutral pH conditions (Figure 4 and Table 1). Our result is in agreement with other studies [39], where they showed rapid degradation of CUR in compounds like vanillin, ferulic acid, etc. [40,41]. It seems donation of hydrogen from acidic phenol group of CUR and formation of the phenolate ion, enables the destruction of CUR at acidic conditions. Kumavat et al., showed the increased stability of the CUR by the conjugated diene structure in acidic pH conditions [41]. It is also possible that the amine groups of CS in acidic environment protonated, which caused the matrix to swells, and facilitate the release of CUR [42]. Overall, the release of CUR from NPs has been discussed in many studies (Table 2). As shown in table 2, the CUR release time (3-12 h) is significantly higher in our study in comparison to previous publications [39,43-45]. Although, the recorded release time is somewhat equal to work performed by Popat et al. [46]. But either due to high concentration of CUR or lose presence of the CUR at surface of NPs, they had burst release time (about 30%) [46]. In our experimental model, since the CUR penetrated into the CS-G complex, the rate of release was slow and constant at varaible time (Figure 4). Hence, it is not exaggerated to say that the release behavior are significantly influenced by the particle size and loading capacity. In a study by Bisht et al. [47], the release of CUR was better than our model, but the carrier they used was toxic. Lastly, we also showed the smaller size particles has faster rate of drug release (Table 1). Moreover, as the loading capacity increased, the internal structure of NPs becomes more compacted. As a result, water could not penetrate into NPs and less diffusion of drug occurred. Thereby, it is possible to adjust the CUR release by changing the particle size and loading capacity and this application is clinically important when one has to control and monitor the release of drug in the *in vivo* conditions.

Conclusion

In most of previous study, the encapsulation of CUR was performed using organic solvent such as chloroform. These

solvents, even at very low amounts, cause a serious risk of human health. In present investigation, we used PEG as CUR solvent. PEG demonstrates acceptable safety profile in long-term use to be included in commercial dosage forms. We showed 2000-fold increases in solubility of CUR in PEG in comparison to water. The loading capacity of CUR in NPs was successfully increased up to 15%. To our knowledge the use of PEG as solvent for CUR has not been reported. This procedure represents a mild and safety process for synthesizing efficient CUR-NPs, as we have not use any organic or toxic solvents.

References

1. Yang F, Lim GP, Begum AN, Ubeda OJ, Simmons MR, Ambegaokar SS, Chen. PP, Kayed R, Glabe CG, Frautschy SA, Cole GM. Curcumin inhibits formation of amyloid β oligomers and fibrils, binds plaques, and reduces amyloid in Vivo J Biol Chem 2005; 280: 5892-5901.

2. Piper JT, Singhal SS, Salameh MS, Torman RT, Awasthi YC, Awasthi S. Mechanisms of anticarcinogenic properties of curcumin: the effect of curcumin on glutathione linked detoxification enzymes in rat liver Int J Biochem Cell Biol 1998; 30: 445-456.

3. Somlak Chuengsamarn MD, Suthee Rattanamongkolgul MD, Rataya Luechapudiporn PHD, Chada Phisalaphong PHD, Siwanon Jirawatnotai PHD Curcumin extract for prevention of type 2 diabetes. Diabetes Care 2012; 35: 2121-2127.

4. Moghadamtousi SZ, Kadir HA, Hassandarvish P, Tajik H, Abubakar S, Zandi KA review on antibacterial, antiviral, and antifungal Activity of curcumin. BioMed Res Inter 2014; 2014: 1-2.

5. Choudhuri T, Pal S, Agwarwal ML, Das T, Sa G. Curcumin induces apoptosis in human breast cancer cells through p53-dependent Bax induction. FEBS Lett 2002; 512: 334-340.

6. Nakamura K, Yasunaga Y, Segawa T, Ko D, Moul JW, Srivastava S. Curcumin down-regulates AR gene expression and activation in prostate cancer cell lines. Int J Oncol 2002; 21: 825-830.

7. Aggarwal S, Takada Y, Singh S, Myers JN, Aggarwal BB. Inhibition of growth and survival of human head and neck squamous cell carcinoma cells by curcumin via modulation of nuclear factor-kappaB signaling. Int J Cancer 2004; 111: 679-692.

8. Anand P, Kunnumakkara AB, Newman RA, Aggarwal BB. Bioavailability of Curcumin: Problems and Promises. Mole Pharma 2007; 4: 807-818.

9. Anand P, Thomas SG, Kunnumakkara AB. Biological activities of curcumin and its analogues (congeners) made by man and Mother Nather. Biochem Pharma 2008; 76: 1590-1611.

10. Kumar A, Ahuja A, Ali J, Baboota S. Conundrum and therapeutic potential of curcumin in drug delivery. Critical Rev Therap Drug Carrier Syst 2010; 27: 279-312.

11. Chaudhary A, Nagaich U, Gulati N, Sharma VK, Khosa RL. Enhancement of solubilization and bioavailability of poorly soluble drugs by physical and chemical modifications: A recent review. J Advance Pharm Edu Res 2012; 2: 32-67.

12. Strickley RG. Solubilizing excipients in oral and injectable formulations. Pharma Res 2004; 21: 201–230.

13. Yalkowsky SH, Rubino JT. Solubilization by cosolvents, Organic solutes in propylene glycol– water mixtures. J Pharma Sci 1985; 74: 416-421.

14. Muller RH, Bohm BHL, Grau J. Nanosuspensions: a formulation approach for poorly soluble and poorly bioavailable drugs. Handbook of Pharmaceutical Controlled Release Technology; 2000b.

15. Muller RH, Jacobs C, Kayer O. Nanosuspensions for the formulation of poorly soluble drugs. Pharmaceutical Emulsion and Suspension, Marcel Dekker, New York, NY, USA; 2000a.

16. Kean T, Thanou M. Biodegradation, biodistribution and toxicity of chitosan. Advance Drug Deliv Rev 2010; 62: 3-11.

17. Wang JJ, Zeng ZW, Xiao RZ, Xie T, Zhou GL, Zhan XR, et al. Recent advances of chitosan nanoparticles as drug carriers. Inter J Nanomed 2011; 6: 765-774.

18. Thanou M, Verhoef JC, Junginge HE. Oral drug absorption enhancement by chitosan and its derivatives. Advance Drug Deliv Rev 2001; 52: 117-126.

19. Thanou M, Verhoef JC, Junginger HE. Chitosan and its derivatives as intestinal absorption enhancers. Advance Drug Deliv Rev 2001; 50: 91-101.

20. Goutam T, Derick R, Ruby rose R. Gelatin based matrices for drug delivery applications, Nova Science Publishers; 2013.

21. Subramanian K, Indumathi S, Vijayakumar V. Fabrication and evaluation of chitosan-gelatin composite film as a drug carrier for in vitro transdermal delivery. IJPSR 2014; 5: 438-447.

22. Nguyen VC, Nguyen VB, Hsieh M. Curcumin-loaded chitosan/gelatin composite sponge for wound healing application. Inter J Polymer Sci 2013; 2013: 1-6.

23. Mollayi S, Tamhidi S, Hashempour H, Ghassempour A. Recycling preparative high performance liquid chromatography for the separation of curcumin from curcuminoids in Curcuma longa L. A Chrom 2015; 27: 1-12.

24. Ghanavi J, Farnia P. Nonviral targeted nanoparticle system for gene transfer and drug delivery. Pending US Patent number 2014/0370500 A1; 2014.

25. Farnia P, Ghanavi J, Bahrami A, Bandehpour M, Kazemi B. Increased production of soluble vascular endothelial growth factors receptor-1 in CHO-cell line by using new combination of chitosan-protein lipid nanoparticles. Int J Clin Exp Med 2015; 8.

26. Farnia P, Ghanavi J, Mollaei S, Bahrami A, Velayati AA. Modification of ChPL (chitosan protein–lipid) nanoparticles for in vitro release of rifampicin (RIF). Inter J Mycobacteri 2015; 4: 16.

27. Fernandes LL, Resende CX, Tavares DS, Soares GA. Cytocompatibility of chitosan and collagen-chitosan scaffolds for tissue engineering. Polimeros 2011; 21: 1-6.

28. Al-Saidi GS, Al-Alawi A, Rahman MS, Guizani N. Fourier transform infrared (FTIR) spectroscopic study of extracted gelatin from shaari (Lithrinus microdon) skin: effects of extraction conditions. Inter Food Res J 2012; 19: 1167-1173.

29. Madhavi M, Madhavi K, Jithan AV. Preparation and in vitro/in vivo characterization of curcumin microspheres intended to treat colon cancer. J Pharm Bioallied Sci 2012; 4: 164-171.

30. Bisht S, Feldmann G, Soni S, Ravi R, Karikar C, Maitra A, Maitra A. Polymeric nanoparticle-encapsulated curcumin ("nanocurcumin"): a novel strategy for human cancer therapy. J Nanobiotech 2007; 5: 1-18.

31. Anuchapreeda S, Fukumori Y, Okonogi S, Ichikawa H. Preparation of lipid nanoemulsions incorporating curcumin for cancer therapy. J Nanotechnol 2012; 2012: 1-12.

32. Seedher N, Bhatia S. Solubility enhancement of cox-2 inhibitors using various solvent systems. AAPS PharmSciTech 2003; 4: 36-44.

33. John MK, Xie H, Bell EC, Liang D. Development and pharmacokinetic evaluation of a curcumin co-solvent formulation. Anticancer Res 2013; 33: 4285-4291.

34. Began G, Sudharshan E, Sankar KU, Appu Rao AG. Interaction of curcumin with phosphatidylcholine: a spectrofluorometric study. J Agric Food Chem 1999; 47: 4992-4997.

35. Yu H, Huang Q. Enhanced in vitro anti-cancer activity of curcumin encapsulated in hydrophobically modified starch. Food Chem 2010; 119: 669–674.

36. Wahlstrom B, Blennow G. A study on the fate of curcumin in the rat. Acta Pharmacol Toxicol (Copenhagen) 1978; 43: 86-92.

37. Taravel MN, Domard A. Collagen and its interaction with chitosan: II. Influence of the physicochemical characteristics of collagen. Biomaterials 1995; 16: 865-871.

38. Taravel MN, Domard A. Relation between the physicochemical characteristics of collagen and its interactions with chitosan. Biomaterials 1993; 14: 930-938.

39. Anitha A, Deepagan VG, Divya Rani VV, Menon D, Nair SV, Jayakumar R. Preparation, characterization, in vitro drug release and biological studies of curcumin loaded dextran sulphate–chitosan nanoparticles. Carbo Polymer 2011; 84: 158–1164.

40. Wang Y, Pan M, Cheng A, Lin L, Ho Y, Hsieh C, Lin J. Stability of curcumin in buffer solutions and characterization of its degradation products. J Pharm Biomed Anal 1997; 15: 1867-1876.

41. Kumavat SD, Chaudhari YS, Borole P, Mishra P, Shenghani K, Duvvuri P. Degradation studies of curcumin. Inter J Pharm Rev Res 2013; 3: 50-55.

42. Jayakumar R, Reis RL, Mano JF. Synthesis and characterization of pH-sensitive thiol-containing chitosan beads for controlled drug delivery applications. Drug Delivery 2007; 14: 9-17.

43. Popat A, Karmakar S, Jambhrunkar S, Xu C, Yu C. Curcumin-cyclodextrin encapsulated chitosan nanoconjugates with enhanced solubility and cell cytotoxicity. Colloid Surface B: Biointer 2014; 117: 520-527.

44. Luis Parize A. Evaluation of chitosan microparticles containing curcumin and crosslinked with sodium tripolyphosphate produced by spray drying Quim Nova 2012; 35: 1127-1129.

45. Mazzarino LI, Borsali R, Lemos-senna E. Mucoadhesive films containing chitosan-coated nanoparticles: a new strategy for buccal curcumin release. J. Pharm. Sci 2014; 103: 3764-3768.

46. Popat A, Karmakar S, Jambhrunkar S, Xu C, Yu C. Curcumin-cyclodextrin encapsulated chitosan nanoconjugates with enhanced solubility and cell cytotoxicity

47. Colloid Surface. B: Biointer 2014; 117: 520-521

48. Bisht S, Feldmann G, Soni S, Ravi R, Karikar C, Maitra A, Maitra A, J. Polymeric nanoparticle-encapsulated curcumin ("nanocurcumin"): a novel strategy for human cancer therapy.Nanobiotech. 2007; 5: 3.

*Correspondence to:

Jalaledin Ghanavi

Mycobacteriology Research Center,
National Research Institute of Tuberculosis and Lung Disease (NRITLD),
Shahid

Beheshti University of Medical Sciences
Tehran
Iran